Medicinal Chemistry Research (2019) 28:1674–1682
https://doi.org/10.1007/s00044-019-02404-7

MEDICINAL CHEMISTRY RESEARCH

ORIGINAL RESEARCH

Structure-based lead optimization to improve the antifungal potency of the tetrahydroimidazo pyridine inhibitors targeted to Candida albicans dihydrofolate reductase and lanosterol 14-alpha-demethylase

Srimai Vuppala[1] · Ramesh Kumar Chitumalla[1] · Bo Sun Joo[2] · Joonkyung Jang[1]

Received: 24 April 2019 / Accepted: 16 July 2019 / Published online: 31 July 2019

Abstract

We investigate the binding and inhibition profiles for a selected dataset of tetrahydroimidazo pyridine molecules against Candida albicans dihydrofolate reductase (DHFR) and lanosterol 14-alpha-demethylase (CYP51). A hit molecule was screened and identified through Lipinski's rule of five, ADMET (absorption, distribution, metabolism, excretion, and toxicity), and the molecular docking. Some inhibitors of our design have shown positive drug scores, good solubilities, and high docking scores over the selected dataset. The first-principles calculation based on the density functional theory was carried out to understand how the electronic distributions of frontier orbitals of molecules affect their inhibition profiles. The present structure-based approach enabled us to design new pharmacophore analogs with improved ADMET profile, drug scores, and docking scores against selected receptors.

Graphical Abstract

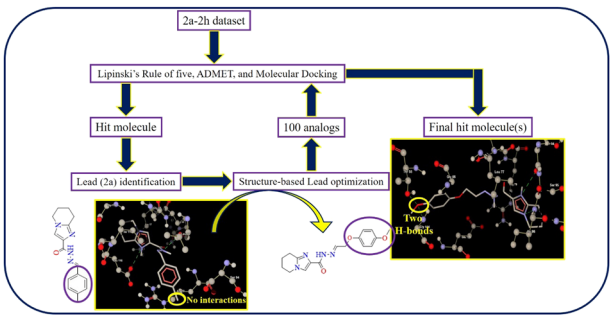

Keywords Density functional theory · Structure-based lead optimization · Candida albicans dihydrofolate reductase · Lanosterol 14-alpha-demethylase · Molecular docking · ADMET

Supplementary information The online version of this article (https://doi.org/10.1007/s00044-019-02404-7) contains supplementary material, which is available to authorized users.

✉ Bo Sun Joo
bosunjoo@hanmail.net

✉ Joonkyung Jang
jkjang@pusan.ac.kr

[1] Department of Nanoenergy Engineering, Pusan National University, Busan 46241, Republic of Korea

[2] Infertility Institute, Pohang Women's Hospital, Pohang 37754, Republic of Korea

Introduction

Recently, fungal diseases significantly increased and became serious threats to human health. Fungal infections can be categorized into two types, superficial and systemic (Di Santo 2010). The former class of infections are less serious (skin and nail infections) and can easily be treated by the existing antifungal drugs. By contrast, the systemic infections are very dangerous especially for the immune-compromised people including AIDS patients (Sheehan et al. 1999; Schiaffella et al. 2005). Many fungal infections, such as neutropenia, endocarditis, endophthalmitis, meningitis, intra-abdominal candidiasis, osteomyelitis, and fungal arthritis, are caused by the opportunistic pathogen Candida albicans (Chimenti et al. 2007). Nowadays, ~46% of fungal endocarditis cases are instigated by Candida albicans (Millar et al. 2005; Negi and Ahmad 2018). Dihydrofolate reductase (DHFR), which catalyzes the reduction of dihydrofolic acid to tetrahydrofolic acid, is a crucial enzyme in the biosynthesis of DNA. DHFR is ubiquitous, i.e., present in both humans and microorganisms. It is complicated to design selective antifungal drugs for DHFR (Chan et al. 1995). On the other hand, the lanosterol 14-alpha-demethylase (CYP51), which belongs to cytochrome P450 family, is another well-known and common antifungal target. The CYP51 is a catalytic enzyme involved in the conversion of lanosterol to ergosterol, a key step in the sterol biosynthesis. The sterols, localized in an integral part of the cell membrane which influences the activity of enzymes and ion channels, are important for regulation of membrane fluidity and permeability (Daum et al. 1998; Abe et al. 2009). Consequently, CYP51 is another prominent antifungal target for researchers.

For fungal infections are not well treated due to the spread of antifungal drug resistance, novel drugs for fungal infections with improved biological activities are highly desired. The azoles, such as voriconazole, fluconazole, and itraconazole, are most widely used antifungal agents (Yamaguchi 1977). Several distinct imidazoles are therapeutically useful antifungal agents with wide spectra against yeasts (Candida albicans). The azoles are also established potent inhibitors of CYP51: they alter the structure of the active site by binding to the heme group of CYP51 and behave like noncompetitive inhibitors (Jefcoate 1978). Herein, by selecting two targets, viz., Candida albicans DHFR and CYP51, we performed an in silico analysis of a selected set of 5,6,7,8-tetrahydroimidazo[1,2-a] pyridine derivatives known to exhibit antifungal activity against Candida albicans (Özdemir et al. 2010).

A structure-based lead optimization has proven to be an efficient computational technique to design and discover a novel drug (Sousa et al. 2006). We screened the selected dataset through Lipinski's rule of five and ADMET (absorption, distribution, metabolism, excretion, and toxicity) (Mabkhot et al. 2016). This was followed by the molecular docking using genetic optimization for ligand docking (GOLD) (Jones et al. 1997; Taha et al. 2015) to identify a hit molecule against the selected receptors. The hit molecule was then considered as a lead for a further optimization study to design new pharmacophore analogs. The lead optimized pharmacophore analogs were further analyzed to identify the most active inhibitor against the selected targets. In addition, the first-principles simulation based on the density functional theory (DFT) was carried out to relate the biological activity of molecules to their electron density distributions of the frontier molecular orbitals. This way, we developed novel pharmacophore analogs with improved drug-likeness properties and inhibition profile against DHFR and CYP51.

Computational details and methodology

Selection of biologically active dataset

We have taken various 5,6,7,8-tetrahydroimidazo[1,2-a] pyridine derivatives known for their antifungal activities (minimum inhibitory concentrations) from the literature (Özdemir et al. 2010). The chemical structures of the selected compounds were prepared and energetically minimized by using the molecular mechanics force field implemented in Hyperchem software (Hypercube 2007, http://www.hyper.com/). The structures and the corresponding biological activities are listed in Table 1.

Structure-activity relationship (SAR) and ADMET properties

The SAR and ADMET properties of the dataset were evaluated by using several computational tools. Molinspiration is a cheminformatics tool that calculates the physicochemical properties and bioactivity scores of drug molecules. Osiris property explorer was employed to calculate properties like ADMET, lipophilicity, solubility (logS), molecular weight, drug-likeness indices, and overall drug scores of ligands. The results of Osiris property explorer are expressed in color codes. In Tables S1 and S4, green, yellow, and red colors indicate low/nontoxic, medium toxic, and highly toxic, respectively. Med Chem Designer 3.0 (Cheng et al. 2012) was used to predict some of the ADMET properties (S + logP, S + logD, Rule of 5).

Target identification, preparation, and active site analysis

The three-dimensional X-ray crystallographic structures of DHFR and CYP51 were retrieved from the protein data

Table 1 Selected molecular structures with inhibitory activities against Candida albicans

Compound	Structure	Inhibitory activity (MIC in mg/mL)
2a	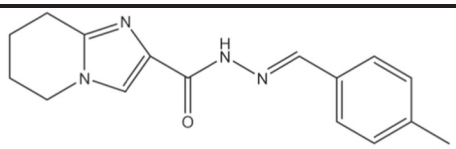	0.032
2b	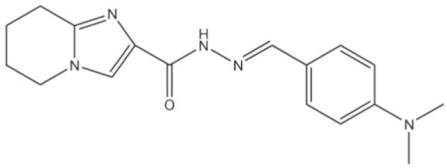	0.125
2c	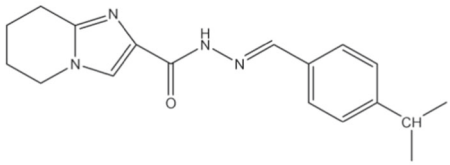	0.125
2d	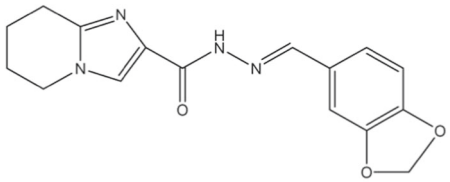	0.063
2e	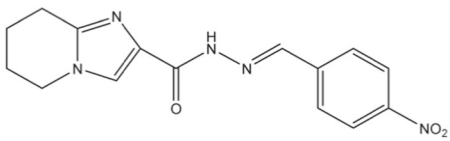	0.125
2f	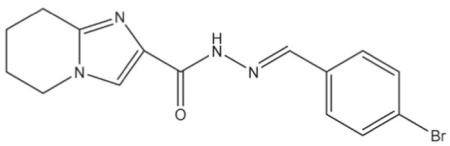	1.000
2g	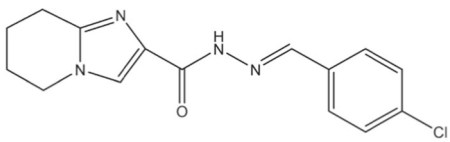	0.125
2h	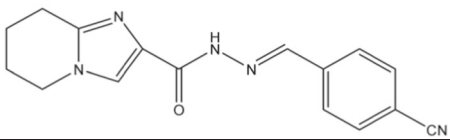	0.032

bank (PDB) at resolutions of 1.85 Å (PDB ID 1AI9) and 1.95 Å (PDB ID 2VKU), respectively. The targets were further prepared by deleting heteroatoms and water molecules. The targets were then optimized with Swiss Protein Database Viewer (SPDBV 4.01) software (Guex and Peitsch 1997) and used for the docking analysis. The active sites of targets were identified by employing SPDBV and ligand explorer of PDB.

Docking software

The target–ligand interaction was examined by using GOLD software. This docking program, utilizing the genetic algorithm to search the ligand and target conformations (Jones et al. 1997), is known to identify the best complimentary pose of a compound for an active site of target. We have fixed the target–ligand interaction distance

and active site radius as 1.5 and 10 Å, respectively. Two scoring functions of GOLD software are the fitness and chem scores. The population size and selection pressure were set to default values in the docking process. Molegro Virtual Docker (Molegro Virtual Docker 2009) was used to visualize the target–ligand interactions.

DFT studies

All the DFT calculations were carried out with Gaussian 09 suite (Frisch et al. 2009). The exchange–correlation function was modeled by using the Becke's three-parameter B3LYP (Becke 1993; Becke 1996) combined with Pople's split valence double-zeta quality basis set with double diffuse functions and double polarization, i.e., 6-311G++(d,p) basis set. The combination of the B3LYP functional with 6-311G++(d,p) basis set are known to accurately minimize the energies of organic pharmacophores (Flores et al. 2018). All the molecules were energetically optimized by using the Berny optimization algorithm. In order to confirm the real minima of the potential energy surface, we performed the frequency calculations at the same level of theory. We carried out the population analysis to unveil the electron density distributions of the frontier molecular orbitals.

Results and discussions

SAR and ADMET properties

The SAR and ADMET properties are crucial for drug design and development. The predictions of molecular physicochemical properties, drug-likeness, and toxicity potentials are important for the computational filtering process. The predicted physicochemical parameters of the selected dataset are listed in Table S1.

The topological polar surface area (TPSA) is closely related to the hydrogen bonding potential of a molecule and is an excellent predictor of the drug transport properties. The TPSAs for the selected dataset ranged from 59.28 to 83.07 $Å^2$, well below the threshold value required for a good transport property, 140 $Å^2$. The molecules with lipophilicity (logP) < 5 have good permeability across the cell membrane. The predicted logP values of all the compounds were less than 5. All the compounds had a low molecular weight (<500) signifying they can be transported, diffused, and absorbed easily. The drug-likeness score is a combined property of logP, logS, molecular weight, and toxicity risks. A positive drug-likeness score indicates a suitability for drug. Molecules **2a** (3.09), **2c** (2.02), **2d** (2.00), and **2g** (2.65) exhibited positive drug scores. On the other hand, molecules **2b** (−2.57), **2f** (−0.02), and **2h** (−6.59) had negative drug-likeness scores. Molecules **2b** and **2d** appeared in red color in the toxicity risk, indicating that these molecules are highly toxic and likely to give undesired effects such as mutagenicity or poor intestinal absorption. Even though all the molecules satisfied the Lipinski's rule of five, some of them had negative drug scores and toxicity risks. Hence, molecule **2a** with the highest drug score was taken to be a good pharmacophore.

Molecular docking analysis

The active sites of DHFR and CYP51 targets (depicted in Fig. S1) were identified by using SPDBV program. The selected compounds were docked into the active sites of targets to explore the binding modes of the inhibitors. The fitness and chem scores of the compounds against DHFR and CYP51 are summarized in Tables S2 and S3.

As per the docking results, the fitness and chem scores of the selected dataset were 49.85–53.36 and 27.87–30.75 against DHFR and 46.97–56.47 and 25.88–29.48 against CYP51, respectively. All the molecules well fitted in the active site grooves of the targets, but only molecule **2a** had desirable ADMET properties and the highest inhibitory activity. Hence, molecule **2a** was taken to be the starting point for further optimization to design novel pharmacophore analogs with improved drug-likeness scores.

The binding structures of molecule **2a** within the active sites of the targets are shown in Figs. 1 and 2. Two nitrogen atoms of molecule **2a** made hydrogen bonds with the active site residues of DHFR, namely Glu116 and Leu76. On the other hand, the keto and methyl groups did not interact with the active site residues. For CYP51, the keto group of molecule **2a** formed a hydrogen bond with Ala256 and the imidazole moiety participated in the hydrophobic interactions with the active site residues such as Met433 (pi-alkyl), Leu321 (pi-alkyl), Arg96 (Pi-cation), Tyr76 (pi-alkyl), Met179 (pi-alkyl), and Heme450 (pi-donor). The docked

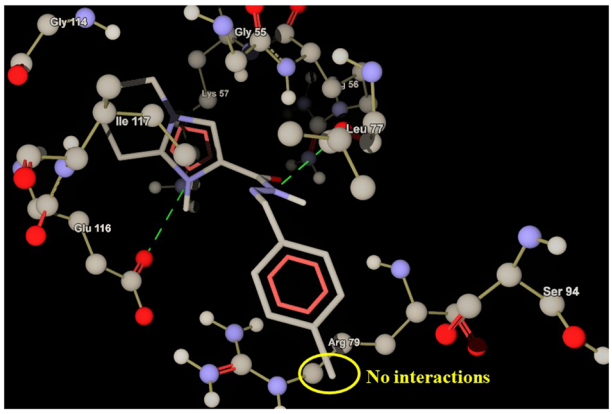

Fig. 1 Binding mode of compound **2a** in the active site of Candida albicans dihydrofolate reductase. Hydrogen bond interactions are shown as green broken lines

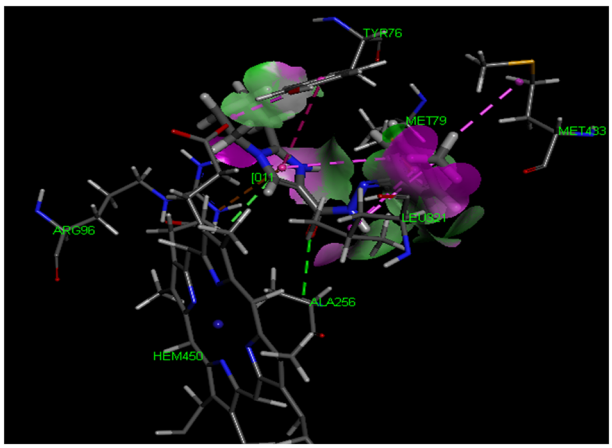

Fig. 2 Binding mode of compound **2a** in the active site of CYP51. Hydrogen bond interactions are drawn as green broken lines. Drawn as pink broken lines are the hydrophobic interactions

complexes of molecule **2a** with the targets were stabilized by forming hydrogen bonds and hydrophobic interactions with the active sites.

The structures (Figs. 1 and 2) of target-ligand (**2a**) complexes showed that the methyl group present on the phenyl ring is not involved in any interaction with the active site residues. Based on the inhibitory activity data of molecules, we observed that an electron donating group on the phenyl ring enhances the inhibitory activity of molecules compared with an electron withdrawing group. Considering these two points above, we carried out structure-based lead optimization studies to design novel potent inhibitors.

Structure-based lead optimization studies

By selecting molecule **2a** as the lead for further optimization, a total of 100 pharmacophore analogs were designed with different substitutions made at their side chains to improve their activities against the selected receptors. The novelty of these molecules was evaluated using SciFinder and PubChem molecule search. Lipinski's rule of five and ADMET properties were predicted for designed molecules and these properties were used as the primary and secondary filters to remove non-drug-like ligands.

Out of 100 designed molecules, only 60 molecules completely satisfied the Lipinski's rule of five and toxicity risks. The optimized molecules **Mol21** (0.03) and **Mol23** (0.03) showed positive enzyme inhibition scores, which confirms that they are biologically active and can exhibit enzyme inhibition properties. The drug-likeness values of optimized molecules (Table S4) were significantly higher than those of the selected dataset. The SAR and ADMET properties of the molecules provided us valuable information regarding the position (ortho, meta, and para) and nature (electron donating or withdrawing) of the substituent on the phenyl ring. These two factors mainly influenced the ADMET profile and inhibitory activity of the molecules. For molecules **2g** and **Mol11** (designed), the positional switching of chlorine atom on the phenyl ring significantly increased the drug-likeness score from 2.65 to 4.45. Similarly, the drug-likeness score increased from 3.31 to 4.65 by the methyl substitution in switching from **Mol7** to **Mol34**. In order to further refine, we identified the best inhibitors by using GOLD. The designed molecules (Fig. S2) with the GOLD fitness scores of more than 50 have the possibility for synthesis.

Binding mode analysis on the optimized molecules against DHFR

In order to scrutinize the binding mode interactions of the optimized molecules, 60 molecules were docked into the active site of DHFR. All the molecules were well fitted into the active site of DHFR, giving fitness scores greater than 42. The docking results of molecules with fitness scores greater than 50 are summarized in Table 2. Seven molecules **Mol19**, **Mol20**, **Mol21**, **Mol22**, **Mol23**, **Mol24**, and **Mol35** showed fitness scores greater than that of their parent pharmacophore.

Figure 3 illustrates the binding interactions of top two optimized inhibitors within the active site of DHFR. **Mol24** scored a fitness score of 59.15 and formed four hydrogen bond interactions with the active site residues of DHFR. Two hydrogen bond interactions were formed between two nitrogen atoms of the imidazole ring and the active site residues Ile96 and Ser94. The methoxy group on the phenyl ring was involved in the other two hydrogen bond interactions with the active site residues Thr58 and Gly114. As shown in Fig. 3, the optimization step of the lead molecule also gave two hydrogen bonds with Ile96 and Ser94 residues, which were not in the region of the active site, so these interactions enhanced the binding affinity of the optimized molecule with neighboring residues. On the other hand, **Mol22** showed a fitness score of 58.48 and hydrogen bond score of 8.15, forming three hydrogen bond interactions with Thr58, Gly114, and Ile117. One of nitrogen atoms of the imidazole and the oxygen atom of the keto group participated in the hydrogen bond interactions. An important structure-activity insight could be obtained by examining the target-ligand complexes of **Mol22** and **Mol24** with DHFR. Each of these two designed molecules had a methoxy group on its phenyl ring at a varying position. The methoxy group of **Mol24** actively joined in the binding interactions with the target but the methoxy group of **Mol22** failed to form such interaction. Therefore, from the docking analysis, it became clear that the positional switching of the methoxy group from C3 (**Mol22**) to C4

Table 2 Molecular docking results of designed pharmacophore analogs against Candida albicans dihydrofolate reductase

Compound	Fitness	Chem score	S(hb_ex)	S(vdw_ext)	DG	S(lipo)
Mol11	51.79	27.09	2.95	38.00	−28.84	114.99
Mol19	58.09	26.61	9.13	39.50	−26.69	105.65
Mol20	57.98	26.43	8.76	40.37	−27.21	109.91
Mol21	60.80	28.33	15.05	39.42	−28.65	105.85
Mol22	58.48	26.72	8.15	41.93	−27.44	118.83
Mol23	56.80	25.78	10.41	38.77	−27.92	163.83
Mol24	59.15	26.39	10.65	40.10	−28.49	164.52
Mol34	52.49	25.56	13.20	33.90	−28.12	134.50
Mol35	56.53	25.68	5.87	42.66	−27.47	143.97
Mol36	53.16	25.85	5.89	38.57	−27.44	123.10
Mol38	52.03	26.79	0.12	43.69	−28.80	137.95
Mol39	51.11	24.13	6.00	37.91	−26.64	121.97
Mol42	52.36	24.15	14.74	34.56	−26.75	126.78
Mol44	51.19	24.44	7.27	38.25	−25.69	122.05
Mol53	53.15	27.49	10.86	36.82	−29.36	124.41

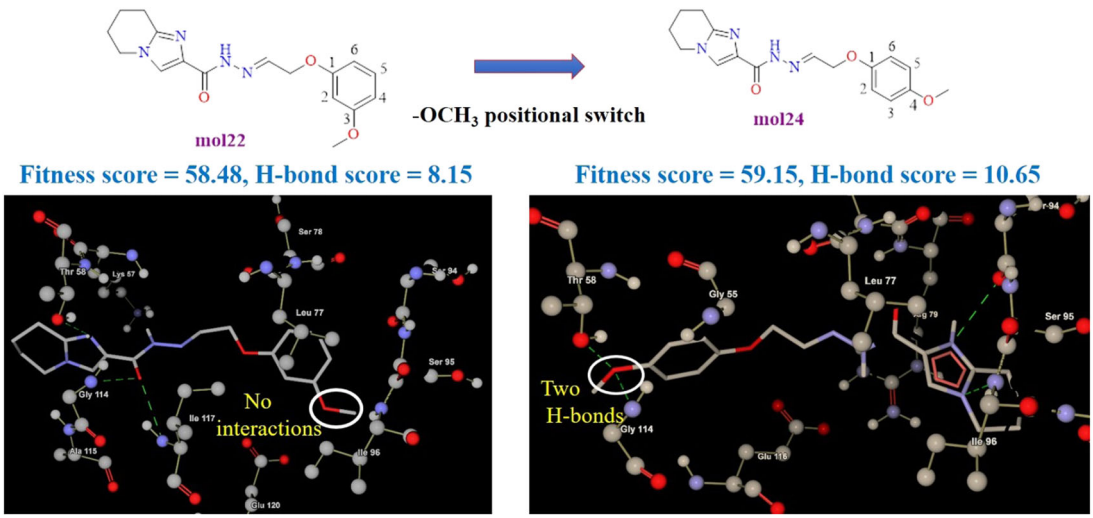

Fig. 3 Binding modes of **Mol22** and **Mol24** in the active site of Candida albicans dihydrofolate reductase. Hydrogen bond interactions are represented as green broken lines

(**Mol24**) on the phenyl ring resulted in an alternative binding orientation with an increased hydrogen bonding interaction.

Binding mode analysis for the optimized molecules against CYP51

All the 60 molecules docked against CYP51 showed good binding affinities. The docking scores of molecules with fitness scores greater than 50 are summarized in Table 3. Total of 13 molecules (**Mol7**, **Mol11**, **Mol20**, **Mol21**, **Mol22**, **Mol24**, **Mol35**, **Mol37**, **Mol38**, **Mol39**, **Mol42**, **Mol44**, and **Mol53**) displayed the fitness scores greater than those of the selected dataset. Two designed molecules **Mol44** and **Mol38** exhibited significant in silico inhibition profiles of the target with fitness scores 59.34 and 56.95 and chem scores 30.46 and 30.61, respectively. The high fitness and chem scores of **Mol44** and **Mol38** could be ascribed to their strong hydrogen bond and hydrophobic interactions (Table 3) with CYP51.

The binding mode of **Mol44** with CYP51 are shown in Fig. 4. The complex of the receptor and ligand was stabilized through the hydrophobic and hydrogen bond interactions within the active site of the target. **Mol44** formed strong hydrogen bond interaction with His259 (hydrogen bond distance of 2.53 Å) and hydrophobic interactions with

Table 3 Molecular docking results of designed pharmacophore analogs against CYP51

Compound	Fitness	Chem score	S(hb_ex)	S(vdw_ext)	DG	S(lipo)
Mol7	56.39	28.56	0.83	46.17	−30.12	208.67
Mol11	54.12	30.16	2.33	42.30	−31.43	194.90
Mol19	50.88	28.07	0.03	41.44	−28.86	200.98
Mol20	53.88	29.91	1.70	44.27	−30.05	212.24
Mol21	53.40	29.16	3.89	43.63	−29.83	195.61
Mol22	54.03	31.37	0.01	45.78	−32.44	212.36
Mol23	50.25	27.02	1.80	41.59	−28.29	211.40
Mol24	53.76	29.83	0.01	44.85	−30.90	203.90
Mol34	53.33	28.35	0.50	44.62	−30.50	211.98
Mol35	55.85	28.78	1.82	46.32	−30.89	218.67
Mol36	51.07	27.12	1.16	40.87	−28.26	188.37
Mol37	54.29	29.27	0.06	45.50	−30.73	212.76
Mol38	56.95	30.61	0.17	47.88	−32.71	230.20
Mol39	54.07	31.02	0.54	44.47	−32.98	260.25
Mol42	54.81	27.71	2.46	42.78	−29.55	203.86
Mol44	59.34	30.46	2.68	46.43	−33.09	238.42
Mol53	53.72	28.95	0.18	43.63	−30.62	184.77

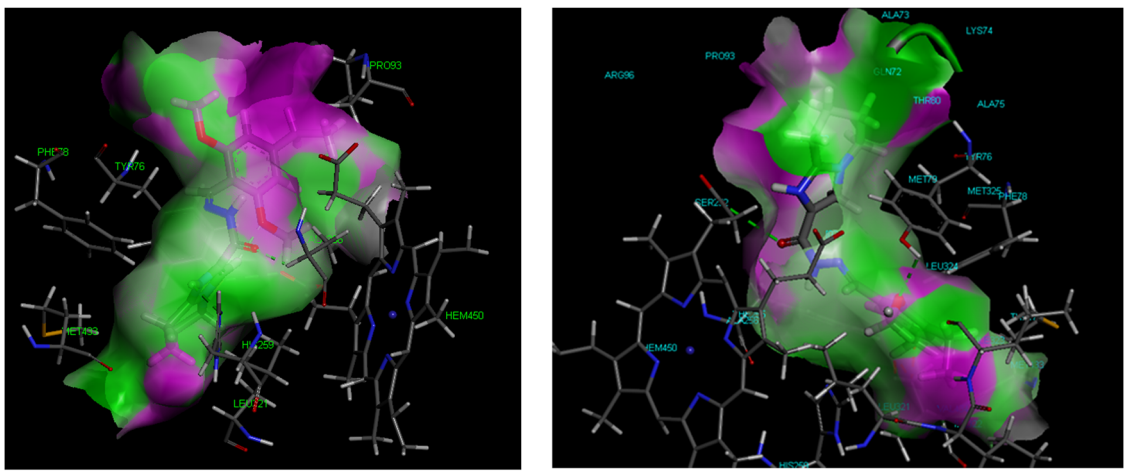

Fig. 4 Binding modes of **Mol44** (left) and **Mol38** (right) in the active site of CYP51. The hydrophobic (hydrophilic) interaction is drawn in pink (green)

Ala256, Met433, Tyr76, Pro93, Heme450, Leu321, and Phe78. On the other hand, **Mol38** (Fig. 4) had a fitness score of 56.95, indicating that the molecule fits well in the entire furrow of the binding site. It formed two hydrogen bonds with Heme450 and Tyr76 and hydrophobic interactions with Ala256, Val434, Ile323, Leu321, Leu324, Met433, and Phe78.

DFT analysis on the frontier molecular orbitals

The in silico investigations above were based on classical mechanics, but a complete understanding of the drug activity should be in principle based on quantum mechanics. The frontier molecular orbitals of ligands are known to play crucial roles in the inhibition process (Voth et al. 2009). It has been known that, for an enhanced drug activity, the highest occupied molecular orbital (HOMO) of the ligand should act as an electron donor, while the lowest unoccupied molecular orbital (LUMO) should act as an electron acceptor (Voth et al. 2009; Xie et al. 2016). We carried out the first-principles calculations utilizing the DFT to relate the inhibitory activities of molecules with their electronic properties in HOMO and LUMO.

As seen in Fig. 5, for molecule **2a**, the electron density in HOMO mainly covered from the methyl-substituted phenyl ring to the region right next to the imidazole moiety. In contrast, the electron density in LUMO is completely shifted to tetrahydroimidazo pyridine ring. The main reason for

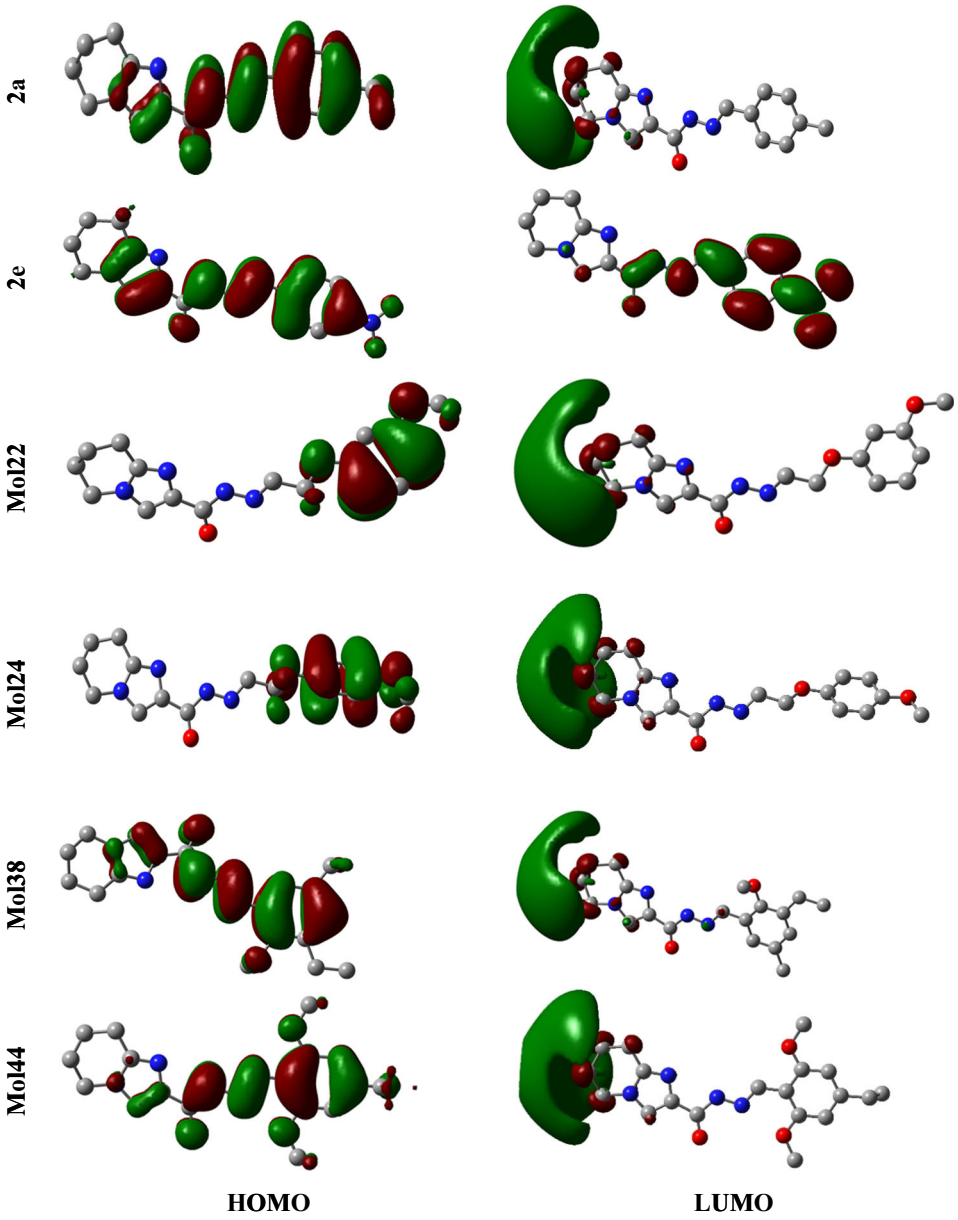

Fig. 5 Electron density distributions of the frontier molecular orbitals obtained by using the DFT calculation at the level of the B3LYP functional with 6-311G++(d,p)

the electron density shifting could be attributed to the electron donating nature of the methyl group on the phenyl ring. On the other hand, for molecule **2e** (less active), the electron density was not significantly shifted from HOMO to LUMO because of the electron withdrawing nature of the nitro group. The lack of donor-acceptor behavior for molecule **2e** led to a less active inhibitor for the selected targets. The electron densities of molecules **2a** and **2e** confirm their active and less-active inhibitions against the selected targets, respectively.

Figure 5 also shows the frontier molecular orbitals of four optimized molecules (**Mol22**, **Mol24**, **Mol38**, and **Mol44**) with good fitness scores. The electron density of HOMO was primarily populated over the methoxy-substituted phenyl ring, whereas that of LUMO was completely shifted to the tetrahydroimidazo pyridine ring. Note that the methoxy substitution on the phenyl ring enhanced the inhibitory activity of the molecules. As explained above, all these active inhibitors had their electron densities of HOMO and LUMO primarily located in the separate regions of their molecular structures.

Conclusion

By selecting a dataset of molecules (**2a**–**2h**) with known inhibitory activities against Candida albicans, we have screened the antifungal dataset by computing their

physicochemical parameters and ADMET properties. The structure-based analysis was carried out to understand the influence of chemical structures on the binding and inhibition profile against two selected receptors, DHFR and CYP51. From the docking analysis on the dataset, a hit molecule (**2a**) was identified and considered as a lead for further structure-based lead optimization. The structure-based optimization step significantly enhanced the binding interactions of the designed compounds with the active sites of the selected receptors. The present optimized compounds were found to have superior drug-likeness and fitness/chem scores compared with those of the selected dataset. The electron density analysis based on the DFT confirmed that the active inhibitors possess an enhanced donor–acceptor nature in their frontier orbitals.

Acknowledgements This study was supported by the National Research Foundation Grants funded by the Korean Government (2018R1A2A2A05019776).

Compliance with ethical standards

Conflict of interest The authors declare that they have no conflict of interest.

References

Abe F, Usui K, Hiraki T (2009) Fluconazole Modulates membrane rigidity, heterogeneity, and water penetration into the plasma membrane in *Saccharomyces cerevisiae*. Biochemistry 48:8494–8504

Becke AD (1993) Density-functional thermochemistry. III. The role of exact exchange. J Chem Phys 98:5648–5652

Becke AD (1996) Density-functional thermochemistry. IV. A new dynamical correlation functional and implications for exact-exchange mixing. J Chem Phys 104:1040–1046

Chan JH, Hong JS, Kuyper LF, Baccanari DP, Joyner SS, Tansik RL, Boytos CM, Rudolph SK (1995) Selective inhibitors of Candida albicans dihydrofolate reductase: activity and selectivity of 5-(arylthio)-2,4-diaminoquinazolines. J Med Chem 38:3608–3616

Cheng F, Li W, Zhou Y, Shen J, Wu Z, Liu G, Lee PW, Tang Y (2012) Admetsar: a comprehensive source and free tool for assessment of chemical ADMET properties. J Chem Inf Model 52:3099–3105

Chimenti F, Bizzarri B, Maccioni E, Secci D, Bolasco A, Fioravanti R, Chimenti P, Granese A, Carradori S, Rivanera D, Lilli D, Zicari A, Distinto S (2007) Synthesis and in vitro activity of 2-thiazolylhydrazone derivatives compared with the activity of clotrimazole against clinical isolates of Candida spp. Bioorganic Med Chem Lett 17:4635–4640

Daum G, Lees ND, Bard M, Dickson R (1998) Biochemistry, cell biology and molecular biology of lipids of *Saccharomyces cerevisiae*. Yeast 14:1471–1510

Di Santo R (2010) Natural products as antifungal agents against clinically relevant pathogens. Nat Prod Rep 27:1084–1098

Flores MC, Márquez EA, Mora JR (2018) Molecular modeling studies of bromopyrrole alkaloids as potential antimalarial compounds: a DFT approach. Med Chem Res 27:844–856

Frisch MJ, Trucks GW, Schlegel HB, Scuseria GE, Robb MA, Cheeseman JR, Scalmani G, Barone V, Mennucci B, Petersson GA, Nakatsuji H, Caricato M, Li X, Hratchian HP, Izmaylov AF, Bloino J, Zheng G, Sonnenberg JL, Hada M, Ehara M, Toyota K, Fukuda R, Hasegawa J, Ishida M, Nakajima T, Honda Y, Kitao O, Nakai H, Vreven T, Montgomery JA, Peralta JE, Ogliaro F, Bearpark M, Heyd JJ, Brothers E, Kudin KN, Staroverov VN, Kobayashi R, Normand J, Raghavachari K, Rendell A, Burant JC, Iyengar SS, Tomasi J, Cossi M, Rega N, Millam JM, Klene M, Knox JE, Cross JB, Bakken V, Adamo C, Jaramillo J, Gomperts R, Stratmann RE, Yazyev O, Austin AJ, Cammi R, Pomelli C, Ochterski JW, Martin RL, Morokuma K, Zakrzewski VG, Voth GA, Salvador P, Dannenberg JJ, Dapprich S, Daniels AD, Farkas Ö, Foresman JB, Ortiz JV, Cioslowski J, Fox DJ (2009) Gaussian 09, revision D.01. Gaussian, Inc., Wallingford, CT

Guex N, Peitsch MC (1997) SWISS-MODEL and the Swiss-Pdb viewer: an environment for comparative protein modeling. Electrophoresis 18:2714–2723

Hypercube Inc. (2007) HyperChem 8.0 package. Hypercube (2007) Inc., Gainesville, FL, USA. http://www.hyper.com/

Jefcoate CR (1978) Measurement of substrate and inhibitor binding to microsomal cytochrome P-450 by optical-difference spectroscopy. Methods Enzymol. 52:258–279

Jones G, Willett P, Glen RC, Leach AR, Taylor R (1997) Development and validation of a genetic algorithm for flexible docking11Edited by F. E. Cohen. J Mol Biol 267:727–748

Mabkhot Y, Alatibi F, El-Sayed N, Al-Showiman S, Kheder N, Wadood A, Rauf A, Bawazeer S, Hadda T (2016) Antimicrobial activity of some novel armed thiophene derivatives and Petra/Osiris/Molinspiration (POM) analyses. Molecules 21:222

Millar BC, Jugo J, Moore JE (2005) Fungal endocarditis in neonates and children. Pedia Cardiol 26:517–536

Molegro ApS (2009) Molegro Virtual Docker, Version 3.2.1. Molegro ApS, Aarhus, Denmark

Negi N, Ahmad A (2018) Current updates on fungal endocarditis. Fungal Biol Rev 32:1–9

Özdemir A, Turan-Zitouni G, Asım Kaplancıklı Z, İşcan G, Khan S, Demirci F (2010) Synthesis and the selective antifungal activity of 5,6,7,8-tetrahydroimidazo[1,2-a]pyridine derivatives. Eur J Med Chem 45:2080–2084

Schiaffella F, Macchiarulo A, Milanese L, Vecchiarelli A, Costantino G, Pietrella D, Fringuelli R (2005) Design, synthesis, and microbiological evaluation of new candida albicans CYP51 inhibitors. J Med Chem 48:7658–7666

Sheehan DJ, Hitchcock CA, Sibley CM (1999) Current and emerging azole antifungal agents. Clin Microbiol Rev 12:40–79

Sousa SF, Fernandes PA, Ramos MJ (2006) Protein–ligand docking: current status and future challenges. Protein Struct Funct Bioinform 65:15–26

Taha M, Ismail NH, Imran S, Selvaraj M, Rahim A, Ali M, Siddiqui S, Rahim F, Khan KM (2015) Synthesis of novel benzohydrazone–oxadiazole hybrids as β-glucuronidase inhibitors and molecular modeling studies. Bioorganic Med Chem 23:7394–7404

Voth AR, Khuu P, Oishi K, Ho PS (2009) Halogen bonds as orthogonal molecular interactions to hydrogen bonds. Nat Chem 1:74

Xie J, Dong H, Yu Y, Cao S (2016) Inhibitory effect of synthetic aromatic heterocycle thiosemicarbazone derivatives on mushroom tyrosinase: insights from fluorescence, 1H NMR titration and molecular docking studies. Food Chem 190:709–716

Yamaguchi H (1977) Antagonistic action of lipid components of membranes from Candida albicans and various other lipids on two imidazole antimycotics, clotrimazole and miconazole. Antimicrob Agents Chemother 12:16–25